Published in final edited form as:
Opt Lett. 2013 March 1; 38(5): 673–675.

High-precision, high-accuracy ultralong-range swept-source optical coherence tomography using vertical cavity surface emitting laser light source

Ireneusz Grulkowski[1], **Jonathan J. Liu**[1], **Benjamin Potsaid**[1,2], **Vijaysekhar Jayaraman**[3], **James Jiang**[2], **James G. Fujimoto**[1], and **Alex E. Cable**[2,*]

[1]Department of Electrical Engineering and Computer Science, Research Laboratory of Electronics, Massachusetts Institute of Technology, 77 Massachusetts Avenue, Cambridge, Massachusetts 02139, USA

[2]Advanced Imaging Group, Thorlabs Inc., 56 Sparta Avenue, Newton, New Jersey 07860, USA

[3]Praevium Research Inc., 5266 Hollister Avenue, Santa Barbara, California 93111, USA

Abstract

We demonstrate ultralong-range swept-source optical coherence tomography (OCT) imaging using vertical cavity surface emitting laser technology. The ability to adjust laser parameters and high-speed acquisition enables imaging ranges from a few centimeters up to meters using the same instrument. We discuss the challenges of long-range OCT imaging. *In vivo* human-eye imaging and optical component characterization are presented. The precision and accuracy of OCT-based measurements are assessed and are important for ocular biometry and reproducible intraocular distance measurement before cataract surgery. Additionally, meter-range measurement of fiber length and multicentimeter-range imaging are reported. 3D visualization supports a class of industrial imaging applications of OCT.

Optical coherence tomography (OCT) has become a valuable tool to visualize the internal structure of semitransparent objects with micrometer resolution [1]. OCT is widely used in biomedicine and is a standard imaging modality in ophthalmology [2]. The typical imaging range of Fourier-domain OCT instruments is from 2 to 6 mm, sufficient for retinal and endoscopic imaging. However, new applications, such as imaging the entire anterior segment, full eye length imaging, ocular biometry, and imaging the upper airway (anatomical OCT), as well as many material imaging applications, require depth ranges of more than 1 cm. [3,4]. Long axial-range measurements have been demonstrated with optical frequency domain reflectometry for characterization of optical fiber components [5].

In spectral/Fourier-domain OCT, the axial imaging range is limited by the spectrometer spectral resolution. Therefore, several full-range techniques were developed for Fourier-domain OCT. However, superior signal roll-off performance can be achieved with swept-source/Fourier-domain OCT (SS-OCT) since the laser linewidth is much narrower than typical spectrometer resolutions. In SS-OCT, the imaging depth range depends on the laser instantaneous linewidth (coherence length), the repetition rate of the sweep, the wavelength tuning range and the detection bandwidth (detector and A/D converter).

*Corresponding author: acable@thorlabs.com.

The SS-OCT imaging range is limited by the finite light source coherence length. Microelectromechanical systems (MEMS) enabled laser-cavity miniaturization, improving coherence properties and the wavelength tuning rate [6]. MEMS tunable vertical cavity surface emitting lasers (MEMS-VCSELs) have recently been recognized as a versatile technology for high-speed, long-range OCT imaging due to their extremely long coherence length (mode-hop-free operation) and the adjustability of both the sweep frequency and the wavelength range [7,8]. These features combined with wide-band detectors and high-speed A/Ds enable SS-OCT imaging beyond the typical OCT depth range. State-of-the-art A/D converters have >gigahertz sampling rates. However, current commercially available cards cannot be optical clocked at much greater than 500 MHz, which limits ultralong-range OCT imaging. Therefore, fixed-frequency gigahertz sampling with sweep recalibration must be used [7].

In this Letter, we demonstrate high-speed ultralong-range SS-OCT imaging using a VCSEL light source. We present several example applications that require precise and accurate measurements of sample parameters derived from volumetric SS-OCT data.

The SS-OCT setup for ultralong-depth-range measurements is shown in Fig. 1(A). The light source was a MEMS-VCSEL (Praevium/Thorlabs, Inc.) driven at different sweep frequencies, lasing near 1075 nm center wavelength. The VCSEL generated an average output power of 18 mW. A long focal length lens (f = 150 or 300 mm, producing spot sizes of 73 and 150 μm and confocal parameters of 8.2 and 37.4 mm) was used in the sample arm and objects were telecentrically scanned. The incident power on the sample was 1.9 mW. A Mach–Zehnder interferometer (MZI) generated a reference fringe signal for OCT signal recalibration [Figs. 1(B) and 1(C)]. The phase of the MZI fringe was extracted in postprocessing and linearized to enable signal resampling in wavenumber (k-space). Both OCT and MZI signals were acquired either by a digitizer (ATS9870, Alazar Inc., 1 GS/s) or oscilloscope (DPO7104, Tektronix, Inc., 1 GHz bandwidth, 5 GS/s). Prototype balanced photodetectors with 1.5 GHz bandwidth (Thorlabs, Inc.) were used. MEMS-VCSEL drive parameters were adjusted to the particular application and the different configurations demonstrated in this study are shown in Table 1. The MZI path difference was 5 mm, 14 mm, 1 m, and 40 mm for operating points A, B, C, and D, respectively. The sensitivity at 50 kHz imaging speed was 105 dB.

We used ultralong-range OCT to perform axial measurements and assess accuracy and precision. Prior to the actual imaging session, the depth range was calibrated. Generally, accuracy describes how close the measurement is to the true (reference) value, and precision describes how close the individual measurements are to each other. The accuracy of the measurement was determined by comparing the mean measured value with a reference value, whereas the precision was evaluated using the standard deviation of the repeated measurements (Table 2). Measurements of optical components (configuration A in Table 1) [Fig. 2(A)] show very good agreement between dimensions from OCT data, manufacturer specifications, and caliper measurement (in parentheses).

Precision and accuracy are also important for ophthalmic biometry measurements. Long-range OCT was demonstrated for *in vivo* human full eye length imaging at 50 kHz A-scan rates with a detection bandwidth limited depth range of 45 mm and axial resolution of 23 μm in tissue (configuration B in Table 1). Volumetric data sets containing 300 × 300 A-scans and spanning 8.5 × 8.5 mm area were acquired. The pupil center was found and the central 100 A-scans (10 × 10 square) were averaged to generate a depth profile [Fig. 2(B)]. Ocular surfaces including the cornea, crystalline lens, and retina were identified and the geometric axial eye length was determined by dividing the intraocular distances by corresponding refractive indices. The results show that there is no statistically significant difference

between measurements with SS-OCT versus a standard FDA-approved commercial clinical biometric device (IOL Master, Carl Zeiss Meditec, Inc.) (Table 2).

Reducing the speed and sweep range enables meter-depth-range measurements (configuration C in Table 1). In this case, the trigger, OCT signal, and calibrating (MZI) signal were acquired using a 1 GHz oscilloscope. An optical fiber patchcord was inserted in one arm of a second MZI interferometer and its length was determined (Table 2) and compared with a length measurement using a ruler.

Extremely long range can be used not only for reflectometry, but also for three-dimensional (3D) visualization of large or deep objects. A 300 mm focal length objective lens was used to provide sufficient depth of focus, and the OCT system operated at 25 kHz A-scan rate (configuration D in Table 1). Figure 3 shows renderings of volumetric data sets (250 × 250 A-scans). Ultralong imaging depth range enabled visualization of a 6 in tall optomechanical element from its top to its base. This example geometry was chosen because it is extremely difficult to perform precise measurements of high-aspect-ratio objects, such as bore holes, using other measurement methods [Fig. 3(A)]. In another example, it was possible to image 9 mm pistol and 5.56 mm rifle bullets located ~8 cm below the surface of a homogeneous gel phantom as well as to identify the bullet type [Fig. 3(B)]. Finally, OCT enabled nondestructive evaluation of nontransparent objects such as white light bulbs [Fig. 3(C)]. 3D volumetric images showing the filament in the light bulb could be obtained through the scattering light bulb glass.

The factors that determine the measurement precision include the axial resolution and performance of the algorithm for extraction of quantitative information from OCT data sets. The accuracy, especially in long-range imaging, is determined by depth calibration of the instrument. Unlike measurements of stationary objects, *in vivo* ophthalmic imaging and ocular biometry measurements have additional variability due to ocular motion making imaging speed important in order to reduce motion error.

Precise measurement is important for ocular biometry (determination of intraocular distances such as axial eye length). Before cataract surgery and replacement of crystalline lenses with intraocular lenses (IOL), axial eye length must be measured. An error of 100 μm results in ~0.25 D error in IOL power calculation, which is the smallest increment of available IOL power. The required length measurement accuracy is 0.5%.

We demonstrated that SS-OCT systems using VCSEL light sources provide a flexible platform for high-speed ultralong-range OCT imaging. The ability to adjust laser operating parameters to work within detector and A/D bandwidth limits enables depth ranges from a few centimeters up to meters using the same instrument. Ultralong-range OCT has the potential to be a useful industrial imaging technique for characterization and inspection of manufacturing processes and quality control. In biomedicine, 3D imaging and mapping can be used in such diverse applications as upper airway imaging, profilometry, and surgical guidance. However, long-range imaging would have a tradeoff in transverse resolution and confocal parameter unless extended focus or Bessel-beam techniques are used.

In conclusion, we demonstrated high-accuracy, high-precision ultralong-range SS-OCT imaging using VCSEL technology. *In vivo* human-eye imaging and visualization of optical and optomechanical components was presented. Additionally, meter-range measurement was shown in optical fibers. SS-OCT enabled imaging of objects immersed in liquids as well as imaging through nontransparent surfaces. Ultralong-range OCT enables completely new applications that were previously impossible.

Acknowledgments

This study is supported in part by the National Institutes of Health (R01-EY011289-26, R01-EY013178-12, R01-EY013516-09, R01-EY019029-03, R01-CA075289-15, R01-NS057476-05, and R44-CA101067-05) and the Air Force Office of Scientific Research (FA9550-10-1-0551 and FA9550-10-1-0063). I. Grulkowski is a visiting scientist from the Institute of Physics, Nicolaus Copernicus University, Torun, Poland.

References

1. Huang D, Swanson EA, Lin CP, Schuman JS, Stinson WG, Chang W, Hee MR, Flotte T, Gregory K, Puliafito CA, Fujimoto JG. Science. 1991; 254:1178. [PubMed: 1957169]
2. Drexler, W.; Fujimoto, JG., editors. Optical Coherence Tomography: Technology and Applications. Springer-Verlag; 2008.
3. McLaughlin RA, Williamson JP, Phillips MJ, Armstrong JJ, Becker S, Hillman DR, Eastwood PR, Sampson DD. Opt. Express. 2008; 16:17521. [PubMed: 18958032]
4. Fercher AF, Mengedoht K, Werner W. Opt. Lett. 1988; 13:186. [PubMed: 19742022]
5. Eickhoff W, Ulrich R. Appl. Phys. Lett. 1981; 39:693.
6. Potsaid B, Baumann B, Huang D, Barry S, Cable AE, Schuman JS, Duker JS, Fujimoto JG. Opt. Express. 2010; 18:20029. [PubMed: 20940894]
7. Grulkowski I, Liu JJ, Potsaid B, Jayaraman V, Lu CD, Jiang J, Cable AE, Duker JS, Fujimoto JG. Biomed. Opt. Express. 2012; 3:2733. [PubMed: 23162712]
8. Jayaraman V, Cole GD, Robertson M, Burgner C, John D, Uddin A, Cable A. Electron. Lett. 2012; 48:1331. [PubMed: 23520409]

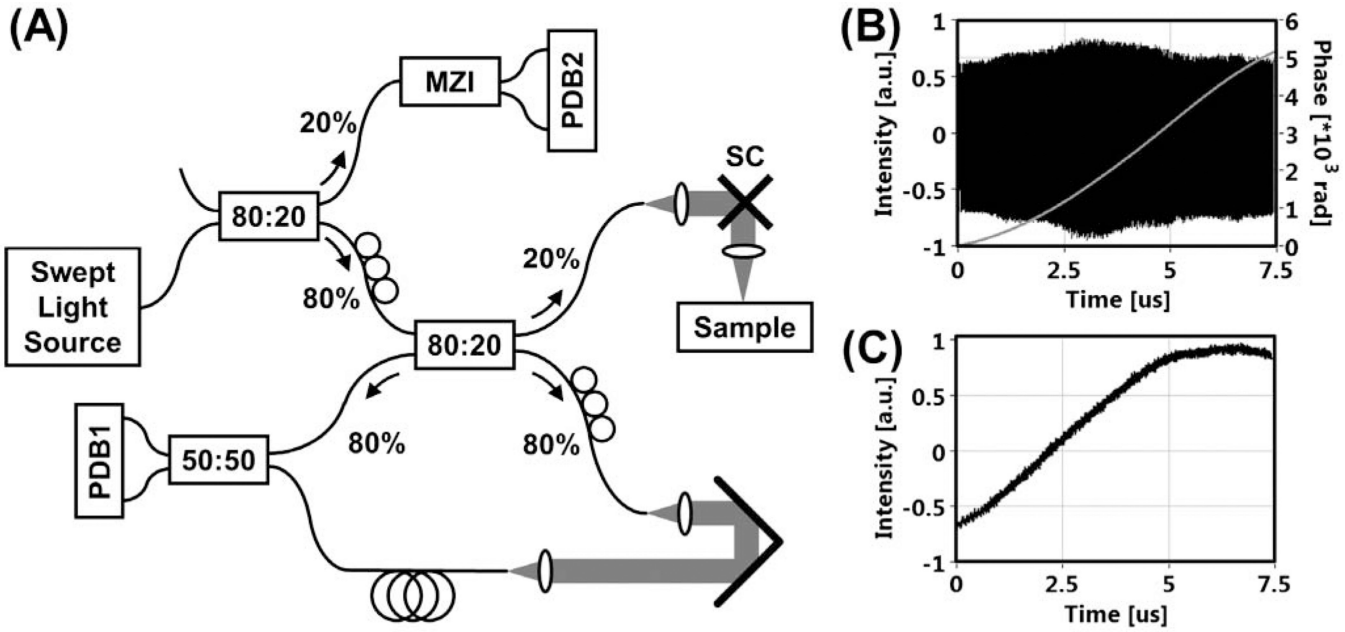

Fig. 1.

Experimental setup. (A) SS-OCT system for long-range imaging. MZI, Mach–Zehnder interferometer; PDB, balanced photodetector; SC, galvanometric scanners. (B) MZI recalibrating signal and (C) example raw OCT signal.

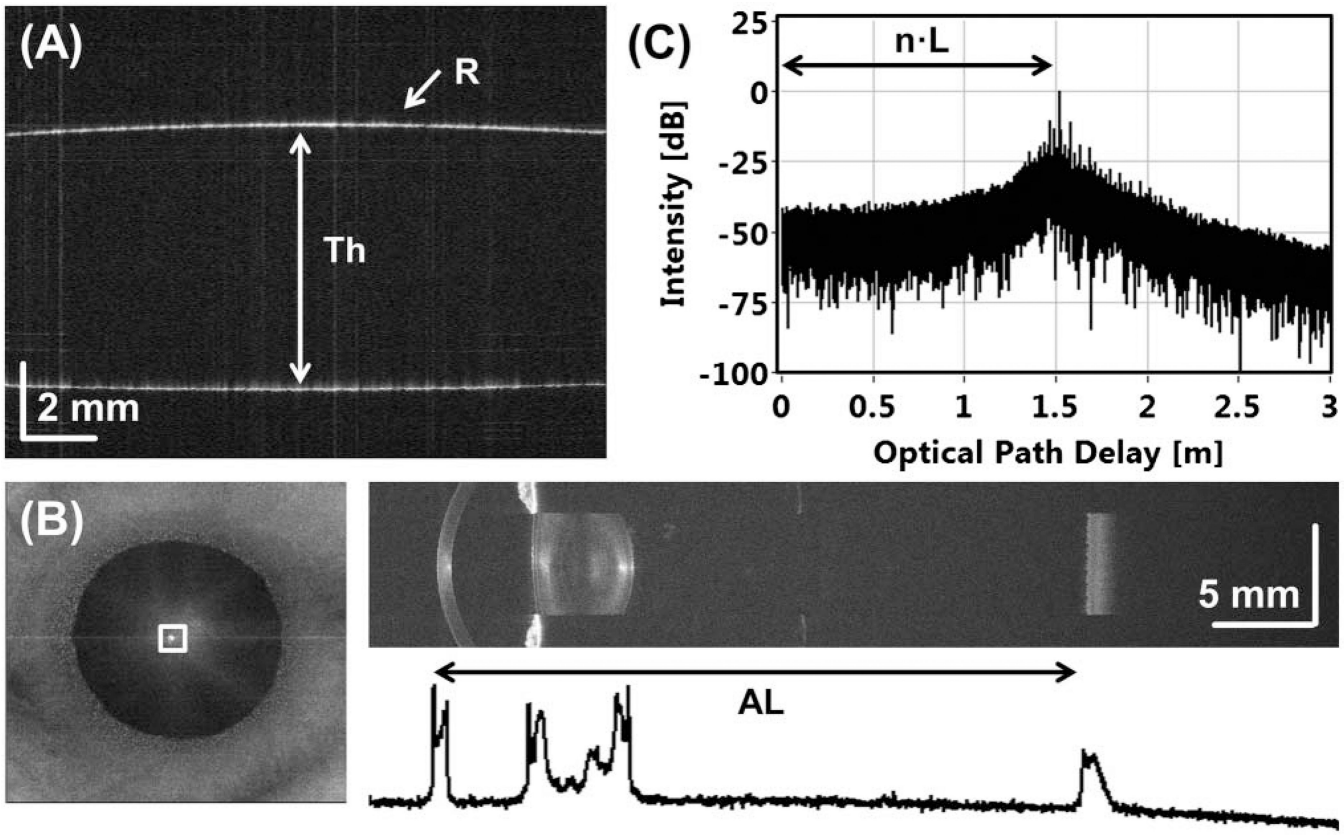

Fig. 2.

Long-range SS-OCT imaging and quantitative measurement. (A) Cross-sectional image of a cylindrical lens enables measurement of central thickness Th and radius R of the surface curvature. (B) Full eye length imaging enables accurate determination of axial eye length AL (ocular biometry). (C) MZI measurement of optical fiber length L (n = 1.4696).

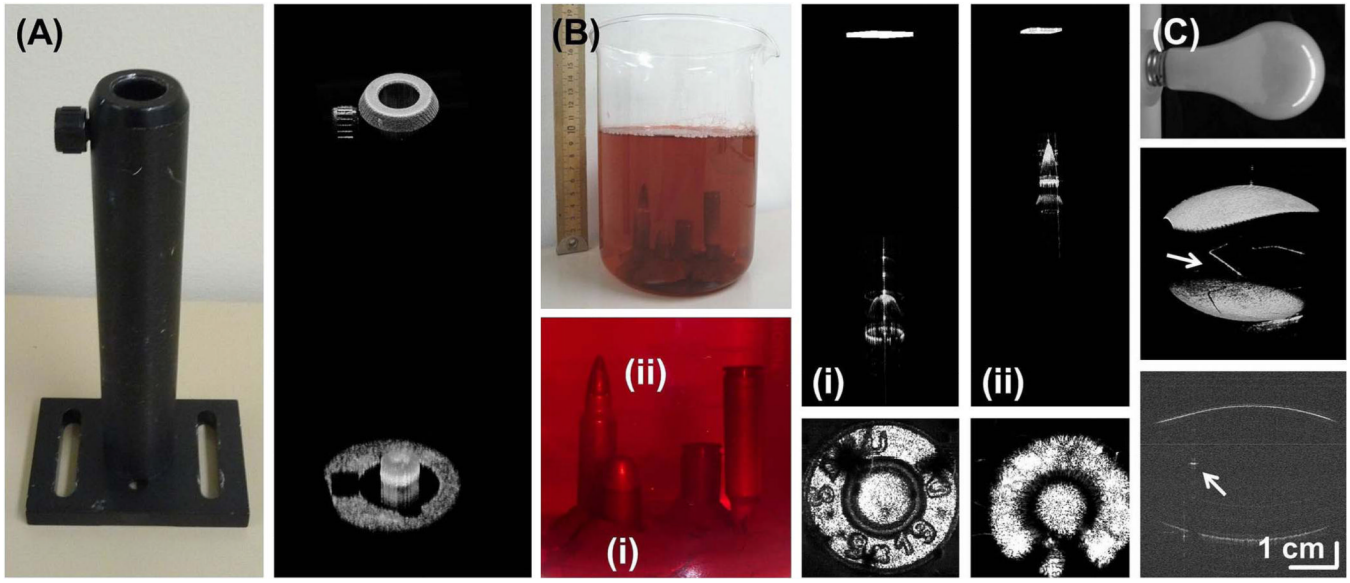

Fig. 3.

(Color online) Ultralong depth-range OCT imaging at 25 kHz A-scan rates. (A) Photograph (left) and 3D reconstruction of volumetric OCT data set (right) of the optical post holder. (B) Ammunition imaging in a gelatin phantom. Photographs of the phantom. Renderings of 9 mm bullet (i) and 5.56 mm rifle bullet (ii) and corresponding *en-face* images showing the rim and primer (bottom). (C) Photograph (top), rendering (middle), and cross-sectional image (bottom) of the white light bulb. The arrows indicate the filament wire.

Table 1

Imaging Configurations Used in the Study

Configuration	A	B	C	D
Imaging speed	100 kHz	50 kHz	20 kHz	25 kHz
Tuning range	27 nm	25 nm	9 nm	25 nm
Axial resolution	25 μm	30 μm	70 μm	30 μm
Depth range (in air)	2.6 cm	6.3 cm	152 cm	15.5 cm
Acquisition	A/D	A/D	Scope	A/D

Table 2

Precision and Accuracy of Quantitative OCT Measurements

Object	Parameter	Measured Value	Reference
Lens	Thickness Th	7.461 ± 0.004 mm	7.28 ± 0.25 mm (7.437 ± 0.010 mm)
	Radius of curvature *R*	77.73 ± 0.49 mm	77.550 mm
Human eye	Axial length AL	25.898 ± 0.022 mm	25.89 ± 0.03 mm
Optical fiber	Length *L*	1.03784 ± 0.00007 m	1.036 ± 0.001 m